

Chain Length Effects for Cluster Ion Formation during High Energy Ion/Surface Collisions with Self-Assembled Monolayer Surfaces

Kurt V. Wolf, David A. Cole,[†] and Steven L. Bernasek*

Department of Chemistry, Princeton University, Princeton, New Jersey 08544, and Evans East, East Windsor, New Jersey 08520

Received: June 5, 2002; In Final Form: July 23, 2002

A high-resolution time-of-flight secondary ionization mass spectrometer (TOF-SIMS) was used to investigate chain length effects for the formation of cluster ions. The clusters were formed from high energy monatomic ion collisions with hydrocarbon self-assembled monolayer (SAM) surfaces that were deposited onto gold substrates. A wide range of *n*-alkanethiols was used to make the SAM surfaces, which included both odd and even hydrocarbon chain length thiols. The mass range of the TOF-SIMS made it possible to monitor all of the cluster ions that were formed by the high energy ion/surface interactions. The focus of this work was on the formation of high mass gold-sulfur and gold-adsorbate cluster ions. Mechanisms for the formation of these large cluster ions are proposed, which build upon a precursor cluster mechanism for high energy collisions with hydrocarbon SAM surfaces.¹ The formation of high mass cluster ions is a function of the chain length of the alkanethiol chemisorbed to the gold surface. It has been demonstrated that both the attenuation of the ions by steric effects and van der Waals interactions dictate their formation.

Time-of-flight secondary ion mass spectrometry (TOF-SIMS) has become an important tool for surface analysis. In both academic and industrial environments, TOF-SIMS is used in combination with traditional surface analytical techniques such as X-ray photoelectron spectroscopy (XPS), Auger electron spectroscopy (AES), and reflection absorption infrared spectroscopy (RAIRS) to provide a detailed analysis of surface structure and composition.² The mass spectra obtained from static SIMS (s-SIMS) typically contain molecular and fragment ion peaks. These ions can be directly related to the structure of the target molecules making SIMS an excellent tool for analysis of organic surfaces. Often when metallic substrates are used, cluster ions are detected in the secondary ion mass spectrum. Uniquely, when an organic thin film is deposited on a metallic surface, a combination of metal-metal, organic, and metal-organic cluster ions are formed.^{1,3,4} Studying cluster formation using a well-characterized system such as self-assembled monolayer (SAM) surfaces can increase our knowledge of the chemical sputtering effects for the SIMS process, dynamic processes of cluster formation via desorption, and possible ion formation mechanisms.

Self-assembled monolayer surfaces are ordered molecular assemblies, which spontaneously form upon the addition of an active surfactant to a suitable substrate. SAM surfaces have been studied intensively in recent years in order to understand their growth and structure, which yields the self-organizing thin film, as well as to utilize the surfaces for technological applications.⁵ Alkanethiols chemisorb spontaneously on Au(111) surfaces to form well-ordered monolayer surfaces.^{6–9} The sulfur headgroup of the *n*-alkanethiol covalently bonds to the gold surface as a thiolate moiety through an inequivalent bonding system where the sulfur headgroup is bridged between two gold atoms.¹⁰ The densest phase, resulting in a coverage close to unity, is referred

to as the standing-up phase, where the hydrocarbon tails of the thiols protrude away from the Au surface. The physical and chemical interactions in the standing-up phase self-organize the thin film so that the backbone of the SAM surface, which is composed of the methylene groups of the alkyl chains, is oriented in an all-trans conformation with an overall chain tilt angle of $\sim 30^\circ$ from the surface normal, as determined by ellipsometry and IR spectroscopy.¹¹ SAM surfaces ranging from $\text{CH}_3(\text{CH}_2)_{10}\text{S}-\text{Au}$ through $\text{CH}_3(\text{CH}_2)_{17}\text{S}-\text{Au}$ appear rigid and the terminal methyl groups also show a high degree of ordering.¹² Figure 1 illustrates two alkanethiols chemisorbed to a gold surface in the standing-up phase. The thiols arrange in a $(\sqrt{3} \times \sqrt{3})R30^\circ$ structure with a $c(4 \times 2)$ superlattice (i.e., $3 \times 2\sqrt{3}$). Nearest-neighbor distances for alkanethiol chains in the standing-up phase for SAM surfaces made from $\text{CH}_3(\text{CH}_2)_9\text{SH}$ or longer thiols are 5.0 Å while the Au-Au atom distances are 2.9 Å.^{13–15} van der Waals interactions stabilize the packing of the thiol tail in the SAM and this stabilization increases as the chain length of the *n*-alkanethiol backbone increases. The well-ordered nature of the gold-thiol network makes this particular class of SAM surfaces very robust, and with minimal defects, the thin films are utilized for many studies.

When studying alkanethiol self-assembled monolayer systems, it was observed that the secondary ion yield using high energy (20 keV) polyatomic primary ions is not significantly greater than the yield obtained using monatomic incident ions.⁴ This is quite unique since polyatomic primary ions typically produce nonlinear enhancements in secondary ion yield when the polyatomic ions are incident on multilayer systems.^{4,16–20} In this study, a liquid metal ion source (LMIS) that produces a well-defined Ga^+ primary ion beam was used, as has been described earlier.³ The purpose of this work was to examine hydrocarbon self-assembled monolayer surfaces in an attempt to understand chain length effects in high energy ion/surface bombardment studies where the largest mass clusters, which formed under these conditions, were detected for each surface.

* Corresponding author. Fax: 609-258-1593. E-mail: sberna@princeton.edu.

[†] Evans East.

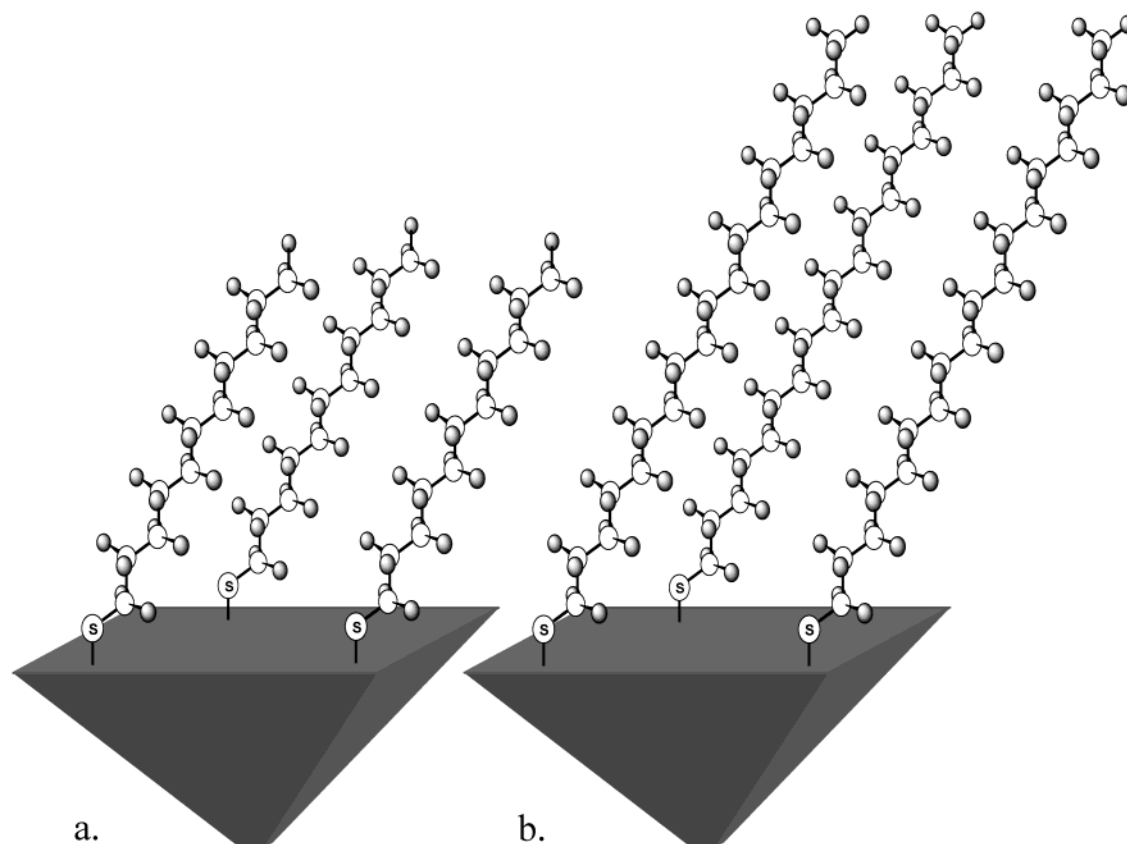


Figure 1. Models of the standing-up phase for (a) 1-undecanethiol and (b) 1-octadecanethiol chemisorbed to a Au surface.

These studies should also help to better understand the dynamic processes that occur during static secondary ion mass spectrometry.

Material and Methods

Gold Substrate. All SAM surfaces were formed on vapor-deposited gold substrates purchased from Evaporated Metal Films of Ithaca, NY. The gold substrates consist of 1000 Å of vapor-deposited Au on 50 Å Ti deposited on silica glass where the surface dimensions are 11/16 in. \times 17/32 in. The Au surfaces were pre-cleaned using a reducing hydrogen flame or an ultraviolet ozone cleaning system (UVOCS).

Materials. Seven *n*-alkanethiols ($\text{CH}_3(\text{CH}_2)_n\text{SH}$, where $n = 10, 11, 13, 14, 15, 16$, and 17) were used in these studies. The thiols were purchased commercially from Aldrich, TCI, and Pfaltz & Bauer, Inc. The $\text{CH}_3(\text{CH}_2)_{16}\text{S}-\text{Au}$ SAM surface was prepared from a mixture of $\text{CH}_3(\text{CH}_2)_{16}\text{SH}$ and $(\text{CH}_3(\text{CH}_2)_{16}\text{S})_2$ which was obtained from Professor David Allara at The Pennsylvania State University.

Monolayer Preparation. Self-assembled monolayer surfaces were prepared by immersing a freshly cleaned Au substrate into a 1 mM absolute ethanol solution of the alkanethiol. Each surface was permitted to grow in the thiol solution for at least two weeks in order for the packing of the thin film to fully equilibrate. The SAM surfaces were rinsed with absolute ethanol. The surfaces were dried, attached to the sample holder, and pumped down to UHV conditions.

Instrumentation. The mass spectra were obtained using a Physical Electronics TFS-2000 TOF-SIMS, which has been described earlier.³ The eight surfaces, seven SAM surfaces and one gold blank, were scanned from mass 1.5 to 5000 for negative secondary ions and from mass 0.5 to 2000 for positive ions. The primary gallium ion beam, with an impact energy of

12 keV for positive ion spectra and 18 keV for negative ion spectra, was rastered over a ($40.3 \mu\text{m} \times 40.3 \mu\text{m}$) area, and each spectrum was acquired over a 15 min period. The mass resolution, $m/\Delta m$, for gold throughout the study remained constant with a value of 8000. The total dose of the primary ions impinging on the surface was found to be $1.7 \times 10^{13} \text{ Ga}^+$ ions/ cm^2 .

Results and Discussion

Cluster ions initiated during high energy ion/surface collisions on alkanethiols chemisorbed on gold are observed in both a greater variety and a higher yield in the detection of negative secondary ions.³ Scanning the extensive mass range carried out in this study, over 3000 cluster ions have been detected and with careful use of isotope ratios, many have been identified exactly. Figures 2 and 3 show the negative ion and positive ion mass spectra for the $\text{CH}_3(\text{CH}_2)_{13}\text{S}-\text{Au}$ SAM surface, respectively. The dominant cluster ions observed are of the type Au_xM_y^- and Au_mS_n^- , where M is defined as the intact thiolate moiety. The high yield of these cluster ions is a result of the strong affinity of gold for sulfur and sulfur containing compounds. Similar studies, which examined self-assembled monolayers on Ag substrates, showed a larger yield for the molecular thiolate and fewer metallic-organic, Ag_xM_y^- , cluster ions.²¹ This is a direct result of the lower affinity of silver for sulfur when compared to gold.⁵ It has been previously observed that the maximum cluster size is a function of the chain length of the alkanethiol attached to the substrate.³ It was observed that the short chain $\text{CH}_3(\text{CH}_2)_{10}\text{S}-\text{Au}$ SAM surface produced intact adsorbate cluster ions up to and including Au_7M_6^- whereas the longer $\text{CH}_3(\text{CH}_2)_{17}\text{S}-\text{Au}$ SAM surface only formed cluster ions upon ion/surface interactions up to and including Au_3M_4^- . It is possible that the longer hydrocarbon chains resist or reflect the

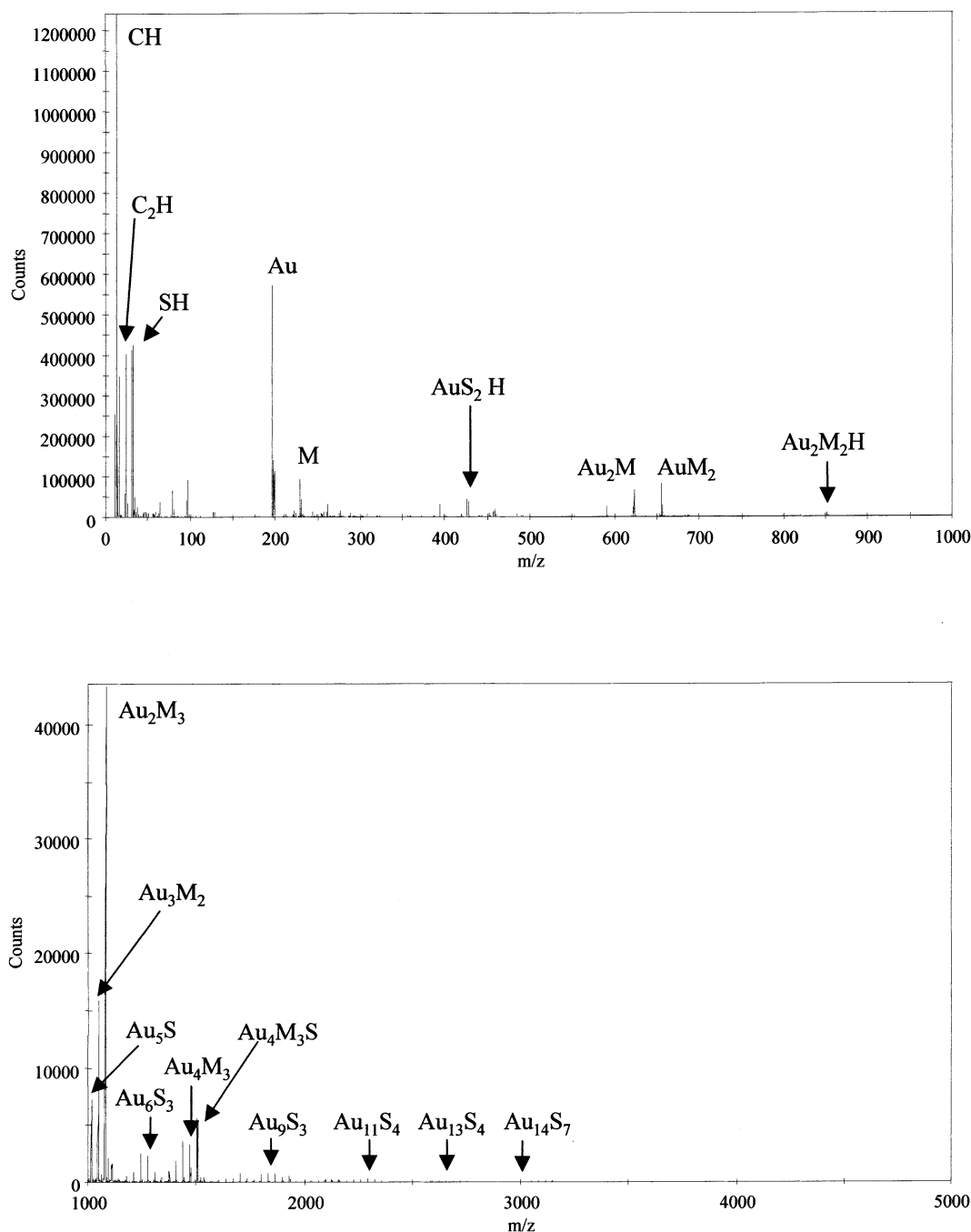


Figure 2. Negative mass spectra for the $\text{CH}_3(\text{CH}_2)_{13}\text{S-Au}$ SAM surface.

incoming primary ions, but the fact that a high energy (18 keV) incident ion was used should limit this process. It has been reported in the literature that small ions penetrate the thin film of SAM surfaces more efficiently.⁴ Therefore the small size of Ga^+ should enhance the secondary ion yield, thus keeping the SIMS process constant for the thin films monitored in this work. Since millions of ion/surface interactions occurred during each primary ion pulse, it is safe to assume that the gallium ions have collided with the thiol chain directly and also targeted the gaps between the chains. For a relatively low flux of primary ions, this results in a large variation in the penetration of the primary ions, which causes numerous independent cascading collision events.

With a primary ion dose of $1.7 \times 10^{13} \text{ Ga}^+$ ions/cm², the SIMS analysis reported here was slightly above the static limit for the system. However, even at this flux of primary ions, the

surface of the system was expected to remain largely unchanged, thus conserving the "static" conditions. To test this concept, the flux of the liquid metal ion source was reduced to 2.7×10^{11} gallium ions/cm², which is well below the static limit, and the SIMS process was repeated. Similar effects were observed for the formation of the cluster ions; however, it was at the cost of a greatly reduced signal-to-noise ratio. Thus it was concluded that the higher primary ion dose was not causing any significant changes to the surface, but the larger signal-to-noise ratio was very beneficial for quantitative observations. It should be noted that at no time was evidence of a crater observed, and it is important to point out that this work was carried out far from the conditions of traditional dynamic SIMS.

The intensity for the cluster ions in the mass spectra follows a logarithmic dependence on chain length of the thiol adsorbed to Au. Figure 4 shows a plot of the log of the ratio $(\text{Au}_x\text{M}_y\text{S}_z\text{H}^- /$

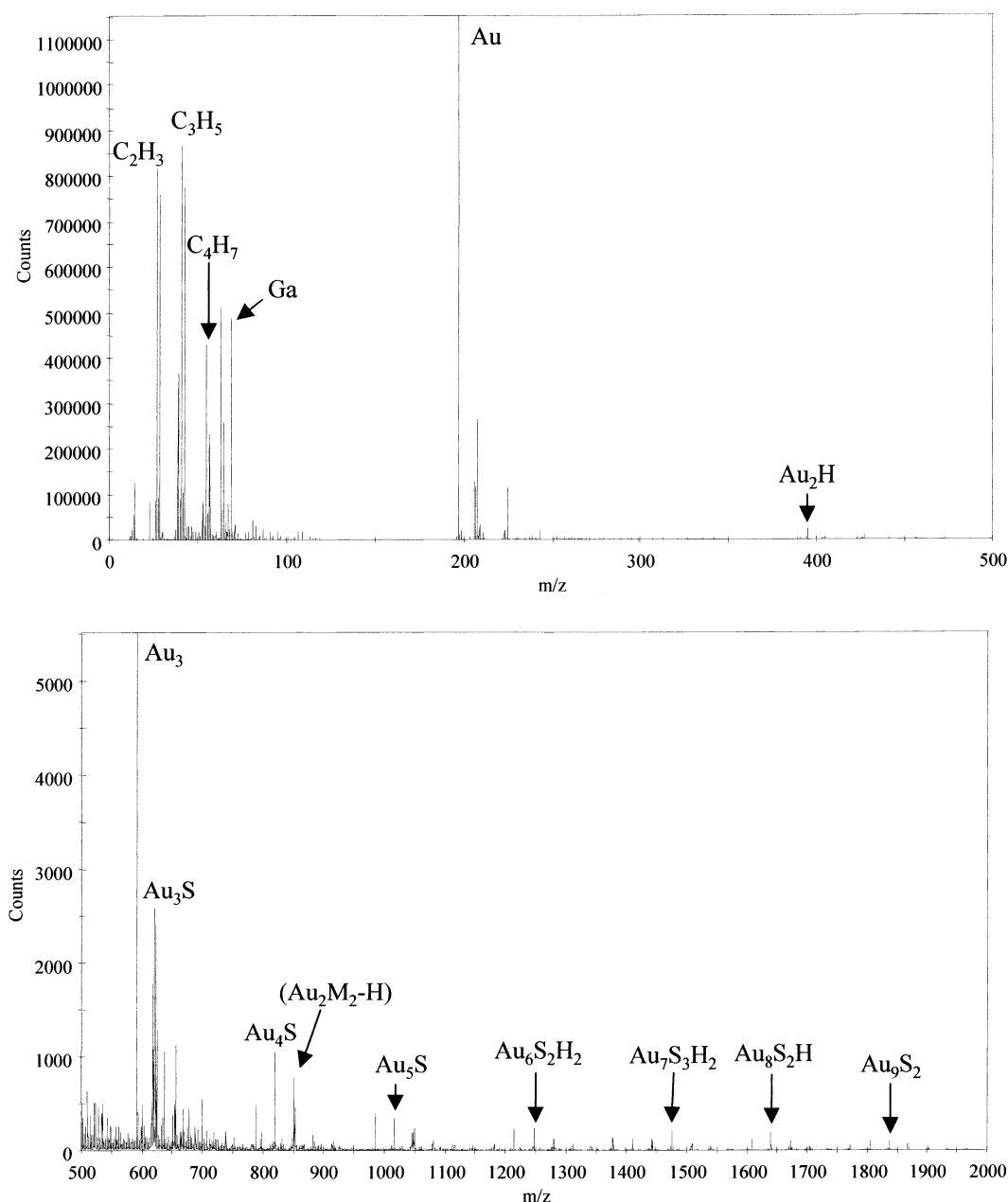


Figure 3. Positive mass spectra for the $\text{CH}_3(\text{CH}_2)_{13}\text{S-Au}$ SAM surface.

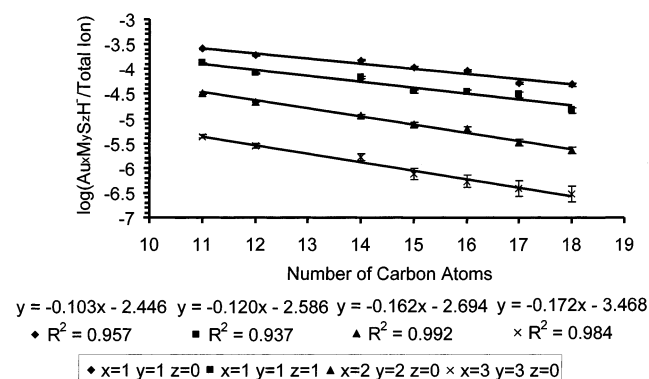


Figure 4. Log plot for the hydrogenated clusters, where x , y , and z are the stoichiometric values for the Au, M, and S species in the cluster, respectively, versus the alkanethiol chain length.

total ion yield) versus the number of carbon atoms in the alkanethiol. This allows each surface and the slopes of the linear least squares lines for the production of specific cluster ions to

be compared as a function of the chain length of the alkanethiol chemisorbed to gold. The total ion yield was chosen for normalization since it did not vary drastically for each surface or acquisition. This is due to the fact that most of the ions in the mass spectra come from alkyl fragmentation due to direct sputtering or unimolecular decomposition of larger ions. Molecular dynamic ion/surface simulations carried out by Liu et al. have demonstrated that the precursor for the formation of the larger clusters is the AuM complex.¹ This mechanism suggests that in order to form larger clusters, such as AuM_2 or Au_2M_2 , adsorbate and/or gold substituents are added to the precursor AuM cluster during the collision cascade.

All of the cluster ions that were observed decreased in intensity with increasing alkanethiol chain length. This trend results from the direct attenuation of the cluster precursor and/or the attenuation of other particles such as gold, sulfur, or the intact thiolate. This trend could be associated with steric effects, which would increase as the alkanethiol chain length of the SAM surface increased in length. However, an important result of

TABLE 1: The Slopes of the Linear Least Squares Fits for Each Cluster Ion as a Function of Chain Length of the Organic Thin Film

cluster ion	slope of linear fit
AuMH ⁻	-0.103
AuMSH ⁻	-0.120
Au ₂ M ₂ H ⁻	-0.162
Au ₃ M ₃ H ⁻	-0.172
Au ₂ M ⁻	-0.141
AuM ₂ ⁻	-0.223
Au ₃ M ₂ ⁻	-0.185
Au ₂ M ₃ ⁻	-0.277
Au ₄ M ₃ ⁻	-0.215
Au ₃ M ₄ ⁻	-0.291

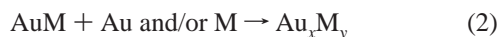
this work is that intermolecular forces between the alkanethiolate chains in the monolayer appear to play a more dominant role in the attenuation of the clusters than was first anticipated.

The cluster ions reported in Figure 4 are unique in the fact that whenever the ratio of the stoichiometric values of Au to M is one, the observed cluster ion is predominantly hydrogenated. This effect has not been discussed even though it has been observed in several preceding studies.^{1,4,21} This observation provides some valuable information when studying ion/surface dynamics. It infers that clusters such as AuM, Au₂M₂, and Au₃M₃ form primarily as stable neutral molecules and the addition of a hydride enables them to be observed in the mass spectra. This effect is represented in Reaction 1,



The positive ion spectra confirm the formation of these neutral species. Again, the 1:1 Au-to-M cluster ions show little to no ion counts. The dominating pathway for the formation of positive cluster ions occurs through the loss of a hydride during the ionization and sputtering process, with cluster ions such as (AuM-H)⁺ being most abundant. Reaction 1 enables further ionization processes to be characterized as will be explained.

Table 1 shows that as the cluster size increases (Au_xM_y⁻, where *x* and *y* are increasing integer values) the slopes of the linear fits become steeper (note the slopes are negative). This suggests a series of consecutive reactions, which strengthens the argument for a precursor cluster mechanism. It is assumed that the AuM cluster is the precursor for the formation of the larger cluster ions, then as the chain length increases, the extent of the general reaction below is limited.



Even the AuMSH⁻ cluster shows a steeper slope, suggesting a possible consecutive reaction pathway with the precursor cluster.

The effect of chain length on the extent of Reaction 2 was studied further by examining other cluster ions that do not have the one-to-one stoichiometry of the cluster ions discussed above. The chain length effects for these cluster ions are shown in Figures 5–7. The simplest case would be the formation of the AuM₂ cluster, and its chain length effect is shown in Figure 5. Since the mass spectra show a larger amount of M⁻ versus AuM⁻ ions, the formation of the AuM₂⁻ cluster ion is best illustrated by Reaction 3, which competes with the formation of the AuMH⁻ cluster ion,



Here a hydrogenated cluster ion is not observed since the product of Reaction 3 is already charged, limiting the addition of a hydride. This was confirmed using isotope ratios where the ion

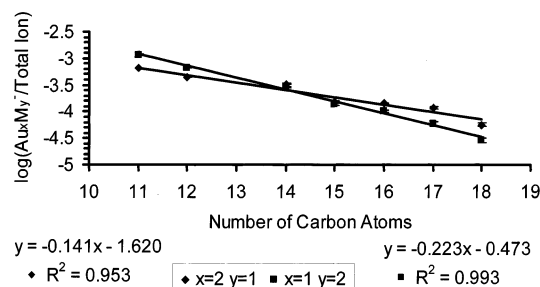


Figure 5. Log plot for the Au₂M⁻ and AuM₂⁻ clusters, where *x* and *y* are the stoichiometric values for the Au and M species in the cluster, respectively, versus the alkanethiol chain length.

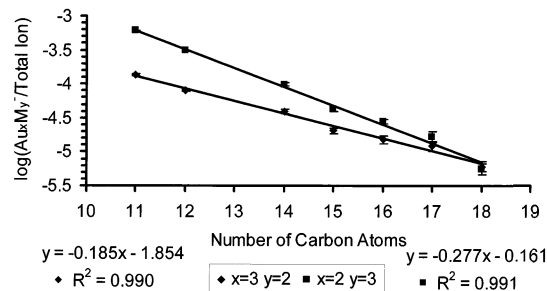


Figure 6. Log plot for the Au₃M₂⁻ and Au₂M₃⁻ clusters, where *x* and *y* are the stoichiometric values for the Au and M species of the cluster, respectively, versus the alkanethiol chain length.

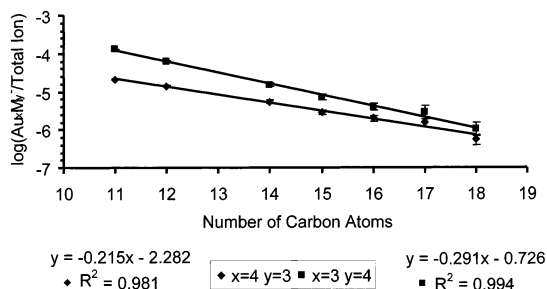


Figure 7. Log plot for the Au₄M₃⁻ and Au₃M₄⁻ clusters, where *x* and *y* are the stoichiometric values for the Au and M species of the cluster, respectively, versus the alkanethiol chain length.

with mass equal to AuM₂+1 corresponded entirely to the AuM₂+1 isotope.³ For comparison reasons, Figure 5 also shows the chain length effects for the formation of the Au₂M⁻ cluster ion, illustrated in Reaction 4,



The positive ion spectra again confirms the ionization mechanisms shown in Reactions 3 and 4, where AuM₂⁺ and Au₂M⁺ ions dominate in ion yield and hydrogenation or dehydrogenation is not observed. Figure 5 illustrates that the cluster ion with the greater number of substituents of the intact adsorbate has a stronger chain length effect resulting in a steeper slope, which is in agreement with the results of Figure 4. Therefore, competition between Reactions 3 and 4 shows a chain length effect where the addition of an adsorbate to the precursor cluster has a greater chain length dependence than the addition of a gold ion. It is proposed that the van der Waals interaction between the alkanethiol chains of the self-assembled monolayer is the cause of this trend. The literature reports a value of 0.07 eV per CH₂ unit for this interaction for *n*-alkanethiol SAM surfaces with a similar number of methylene groups as used in this work.^{5,11} Due to the van der Waals interactions, it is apparent

that the longer chain length films are bound more tightly than the corresponding shorter chain length thiols on gold. Therefore, in order for the intact adsorbate molecule to exit the organic film, the van der Waals force would have to be overcome. Since the energy available is fixed by the collision energy of the primary ion, the ion yield of the cluster ions will decrease as the alkanethiol chain length increases. This effect is illustrated clearly in the comparison of Figure 1, parts a and b, with Figure 5.

SIMS on a standing-up phase SAM surface would require not only the breaking of covalent and metallic bonds but would also include overcoming the dispersion forces between the chains in order to release an intact adsorbate. The van der Waals interaction would have a direct effect since molecular dynamics calculations show the dominating desorption trajectory for an intact adsorbate occurs when the gold-adsorbate complex (AuM) lifts upward, perpendicular to the surface normal.¹ Following this mechanism, Figure 1 shows that the longer hydrocarbon chain monolayer would resist this process more than a shorter hydrocarbon chain because a greater number of chain-chain interactions would have to be broken. This explains why the extent of Reaction 3 is limited more than Reaction 4 as the hydrocarbon chain length of the alkanethiol on gold is increased. This mechanism may also apply to the formation of Au_mS_n^- cluster ions. However, the formation of these cluster ions is generally much more complex since different degrees of hydrogenation are observed making it difficult to accurately assign reaction pathways.³ The general decreasing slope for all cluster ions as a function of chain length observed is due to the increasing steric hindrance the escaping ions must overcome as the chain length increases. Table 1 shows that the slope of the AuMSH^- cluster ion is steeper than that for the AuMH^- cluster ion, likely due to the attenuation of SH^- versus H^- by the thin film and in this case the reaction between sulfur and hydrogen.

Figures 6 and 7 show the chain length dependence of even larger mass cluster ions. Figure 6 again demonstrates that the cluster ion with the larger integer value of M decreases more in intensity, as the chain length of the thiol backbone increases in length, as compared to the gold-dominated cluster ion. Likewise, the formation of the largest cluster ion observed in all seven thin films, the Au_3M_4^- cluster ion, follows the same trend (Figure 7). Since the chain length effect is conserved through the formation of all Au_xM_y^- cluster ions, and is observed for all seven SAM surfaces, it can be concluded that the van der Waals interactions between the alkanethiol chains limits the formation of the adsorbate rich cluster ions. The increase in the length of the hydrocarbon backbone chain of the alkanethiol on gold results in an increase in the intermolecular interactions. For the larger cluster ions, it is difficult to infer the combination and/or recombination mechanisms of ions and neutrals which yield the anions that are detected in the mass spectra. However, the precursor mechanism for the formation of clusters proposed by Liu et al. is consistent with the chain length dependence observed here.¹ Liu et al., also demonstrated the most probable desorption trajectory occurs perpendicular to the surface plane for the departing clusters.¹ At low fluxes of primary ions, at or around the static limit, this trajectory would enhance the effects of breaking the van der Waals interactions resulting in a distinct chain length effect, which agrees very well with the results of this work.

Conclusions

TOF-SIMS has proven to be a very useful method for studying SAM surfaces. This technique offers a means to detect

all of the cluster ions that are formed under high energy ion/surface interactions. This was possible due to the high mass limit characteristic of the TOF mass analyzer. In this study TOF-SIMS was successfully used to compare the high mass cluster ions that are formed during high energy ion/surface collisions on varying chain length self-assembled monolayer surfaces. The chain length of the SAM surface drastically influences the ion yield of the large mass cluster ions. Many reaction pathways are introduced, leading to a much broader understanding of high energy ion/surface interactions which are characteristic of static SIMS. Building on past work using molecular dynamic simulations by Liu et al., the precursor cluster model explains the experimental data for the formation of high mass cluster ions.¹ The concept of ion attenuation as a function of film thickness was confirmed, but more interestingly, the effects of intermolecular forces also appear to strongly influence the formation of the cluster ions. This intermolecular effect was clearly demonstrated, where the cluster ion with the largest number of intact adsorbates continually showed a stronger chain length dependence than the corresponding gold-rich adsorbate cluster ions.

Acknowledgment. We thank Dr. Xia Dong for her assistance and advice for the SIMS analyses, Professor David Allara for material to produce the $\text{CH}_3(\text{CH}_2)_{16}\text{S}-\text{Au}$ SAM surfaces, and Professor Barbara Garrison for discussions concerning preliminary results. We are also grateful for the support of this work by the National Science Foundation, Division of Chemistry.

References and Notes

- (1) Liu, K. S. S.; Yong, C. W.; Garrison, B. J.; Vickerman, J. C. *J. Phys. Chem. B* **1999**, *103*, 3195.
- (2) Schwieters, J.; Cramer, H. G.; Heller, T.; Jurgens, U.; Niehuis, E.; Zehnpfenning, J.; Benninghoven, A. *J. Vac. Sci. Technol. A* **1991**, *6*, 2864.
- (3) Wolf, K. V.; Cole, D. A.; Bernasek, S. L. *Anal. Chem.*, in press.
- (4) Harris, R. D.; Baker, W. S.; van Stipdonk, M. J.; Crooks, R. M.; Schweikert, E. A. *Rapid Commun. Mass Spectrom.* **1999**, *13*, 1374.
- (5) Schreiber, F. *Prog. Surf. Sci.* **2000**, *65*, 151.
- (6) Nuzzo, R. G.; Allara, D. L. *J. Am. Chem. Soc.* **1983**, *105*, 4481.
- (7) Nuzzo, R. G.; Fusco, F. A.; Allara, D. L. *J. Am. Chem. Soc.* **1987**, *109*, 2358.
- (8) Porter, M. D.; Bright, T. B.; Allara, D. L.; Chidsey, C. E. D. *J. Am. Chem. Soc.* **1987**, *109*, 3559.
- (9) Bain, C. D.; Troughton, E. B.; Tao, Y. T.; Evall, J.; Whitesides, G. M.; Nuzzo, R. G. *J. Am. Chem. Soc.* **1989**, *111*, 321.
- (10) Vargas, M. C.; Giannozzi, P.; Selloni, A.; Scoles, G. *J. Phys. Chem. B* **2001**, *105*, 9509.
- (11) Nuzzo, R. G.; Dubois, L. H.; Allara, D. L. *J. Am. Chem. Soc.* **1990**, *112*, 558.
- (12) Wolf, K. V.; Cole, D. A.; Bernasek, S. L. *Langmuir* **2001**, *17*, 8254.
- (13) Ulman, A. *An introduction to ultrathin organic films from Langmuir-Blodgett to self-assembly*; Academic Press: San Diego, 1991.
- (14) Dubois, L. H.; Nuzzo, R. G. *Annu. Rev. Phys. Chem.* **1992**, *43*, 437.
- (15) Finklea, H. O. *Electroanalytical Chemistry*; Bard, A. J., Rubinstein, I., Eds.; Marcel Dekker: New York, 1996; 19, 109.
- (16) Appelhans, A. D.; Delmore, J. E.; Dahl, D. A. *Anal. Chem.* **1987**, *59*, 1685.
- (17) Appelhans, A. D.; Delmore, J. E. *Anal. Chem.* **1989**, *61*, 1087.
- (18) Delmore, J. E.; Appelhans, A. D. *Biol. Mass Spectrom.* **1991**, *20*, 237.
- (19) Park, M. A.; Cox, B. D.; Schweikert, E. A. *J. Chem. Phys.* **1992**, *96*, 8171.
- (20) Ingram, J. C.; Groenewold, G. S.; Appelhans, A. D.; Delmore, J. E.; Dahl, D. A. *Anal. Chem.* **1995**, *67*, 187.
- (21) Vickerman, J. C.; Briggs, D.; Henderson, A. *The Static SIMS Library*; Surface Spectra Ltd.: Manchester, U.K., 1997.